

## Effect of Urografin on the Kidney of Adult Female Albino Rat and the Possible Protective Role of Nebivolol: A Morphological and Ultrastructural Study

Mohamed Emad<sup>1</sup>, Al-Moatassem-Bellah Mohamed El-Sherif<sup>1</sup>, Maha Khaled Abd-El Wahed<sup>2</sup> and Radwa Mohammed Ahmed<sup>2</sup>

Anatomy and Embryology Departments, Faculties of Medicine, Cairo University<sup>1</sup> and Fayoum University<sup>2</sup>.

[dr.mahakhalid@yahoo.com](mailto:dr.mahakhalid@yahoo.com)

**Abstract: Background:** Contrast-induced nephropathy (CIN) means impairment of renal functions occurring within 48-72 hours following intravascular administration of contrast media with the absence of alternative cause. Urografin is one of the most commonly used high-osmolar contrast agents. It induces its nephrotoxic effects via different mechanisms. Nebivolol is a selective  $\beta_1$ -adrenergic receptor antagonist, used as a prophylactic agent for CIN for several reasons. The present work was designed to study the histological and ultrastructural changes in the kidney of the adult female albino rat following intravenous administration of urografin and the possible protective role of nebivolol if used concomitantly with urografin. **Material and Methods:** Fifty adult female albino rats were used in this study. They were divided into five groups, ten rats each; group I (normal control), group II (dehydrated sham) dehydrated for 3 days, group III (dehydrated nebivolol treated) dehydrated for 3 days and received nebivolol by oral route at a daily dose of 2 mg/kg for 5 days, group IV (dehydrated contrast medium administration) dehydrated for 3 days and injected urografin intravenously at a dose of 6 ml/kg at day 4, group V (dehydrated contrast medium and nebivolol administration) dehydrated for 3 days, received nebivolol by oral route at a dose of 2 mg/kg for consecutive 5 days and injected urografin intravenously at a dose of 6ml/kg at day 4. Twenty four hours after the end of the experiment, all animals were sacrificed by cervical decapitation. Both kidneys were excised and prepared for either light microscopic or transmission electron microscopic studies. **Results:** Administration of urografin to dehydrated rats resulted in severe nephrotoxic changes both in cortex and medulla. These findings were supported by ultrastructural study of glomeruli, proximal convoluted tubules and medullary thick ascending loop of Henle. Concomitant administration of nebivolol afford a partial protection to renal glomeruli and the renal tubules. **Conclusion:** Urografin administration caused significant alterations in the renal histological structure. Concomitant administration of nebivolol affords a partial protection against urografin-induced nephrotoxicity due to its vasodilator and antioxidant effects. It can be recommended to use nebivolol to protect against urografin-induced nephropathy especially in patients who undergo coronary angiography.

[Mohamed Emad, Al-Moatassem-Bellah Mohamed El-Sherif Maha Khaled Abd-El Wahed and Radwa Mohammed Ahmed. **Effect of Urografin on the Kidney of Adult Female Albino Rat and the Possible Protective Role of Nebivolol: A Morphological and Ultrastructural Study.** *Life Sci J* 2013;10(4):248-261]. (ISSN: 1097-8135). <http://www.lifesciencesite.com>. 33

**Key Words:** Contrast-induced nephropathy, Urografin, Nebivolol, Kidney, Female rats.

### 1. Introduction:

Contrast-induced nephropathy (CIN) means impairment of renal functions occurring within 48-72 hours following intravascular administration of contrast media with the absence of alternative cause (*Fishbane et al., 2004*).

CIN is the third leading cause of hospital acquired renal failure and is associated with significant morbidity and mortality. Chronic kidney disease is the primary predisposing factor for CIN. Other risk factors include dehydration status, the type and amount of contrast and the use of concomitant nephrotoxic agents (*Schweiger et al., 2007; Santos et al., 2011*).

Contrast media are divided into high-osmolar, low-osmolar and iso-osmolar media (*Persson et al., 2005*). One of the most commonly used high-osmolar contrast agents is urografin (diatrizoate). It induces its

nephrotoxic effects via different mechanisms such as outer-medullary hypoxia secondary to renal artery vasoconstriction, direct tubular toxicity, tubular obstruction, high osmolality of the contrast medium and oxidative stress (*Detrenis et al., 2005*).

Proximal convoluted tubular cells (PCT) and cells of medullary thick ascending limb of Henle (mTAL) are particularly vulnerable to direct urografin nephrotoxicity. Urografin selectively causes ischemia in the deeper portion of the outer medulla, an area with high oxygen requirements and remote from vasa recta supplying the renal medulla with blood (*Merten et al., 2004; Persson et al., 2005*).

*Huang et al. (2003)* reported that haemolysis and haemoglobinuria occur following urografin injection and acute renal failure may supervene. Also, red blood cells aggregation may occur in the presence of a high concentration of urografin. Hypertonicity of

hypertonic contrast media leads to red blood cell rigidity because water leaves the interior of the cells by osmosis and the red blood cells become rigid. *Wong et al.(2012)* suggested that renal tubular obstruction following contrast injection is due to increased viscosity of urine, precipitation of Tamm Horsfall glycoprotein forming casts and sloughed cells incorporated in these casts, worsening intra-tubular obstruction.

Current recommendations to decrease the risk of CIN include hydration with intravenous isotonic saline, avoiding high osmolar and high volume of contrast media and avoiding nephrotoxic drugs. N-acetylcysteine, ascorbic acid and sodium bicarbonate treatments are fairly benign (*Jo et al., 2009; Teplan, 2012; Burchardt et al.,2013*).

Small randomized trials for the use of various vasodilators, including dopamine,  $\beta$ -blockers or prostaglandin E<sub>1</sub> have not been shown to reduce the risk of CIN in comparison with fluid therapy(*Brendan et al., 2006*).

Nebivolol, a last-generation beta blocker, is a selective  $\beta_1$ -adrenergic receptor antagonist, used as a prophylactic agent for CIN for several reasons. It leads to an increase in the renal nitric oxide excretion, a significant increase in the renal plasma flow and glomerular filtration rate, reduced proteinuria, suppression of the renin-angiotensin aldosterone system and inhibition of angiotensin II and endothelin-1 (*Mason et al., 2006; Gupta & Wright, 2008*). Additionally, nebivolol decreases oxidative stress biomarkers and induces a substantial reduction in the accumulation of extracellular matrix proteins and fibrosis(*Toblli et al.,2011*).

Furthermore, *Avci et al.(2011)* pointed out that the most common procedure associated with CIN is coronary angiography, which may cause significant fluid and ion shift into blood vessels leading to hypertension. Most of the patients who undergo coronary angiography have indication for the use of nebivolol for one week at a dose of 5 mg per day because it has anti-hypertensive, anti-ischemic and anti-oxidant effects in the coronary arteries of patients with hypertension.

Female sex is a frequently cited but somewhat controversial risk factor for contrast-induced nephropathy. A more recent study suggested that women may have unfavorable baseline characteristics (more frequent hypertension and diabetes, lower baseline kidney functions, hereditary factors, estrogens, platelets aggregation, low hematocrit value) that put them at risk for CIN (*Mueller et al.,2004*).

The aim of the present work was to elucidate the morphological and ultrastructural alterations resulting from urografin administration in the kidney of adult female albino rat and to investigate the

possible protective role of nebivolol against urografin - induced nephropathy.

## 2. Material and Methods

### Material:

#### Animals and experimental design:

Fifty adult female albino rats weighing 180-220 g were used in this study. They were obtained from the animal house, Faculty of Medicine, Cairo University. The rats were housed in separate cages (5 rats in each cage) and maintained under standard laboratory and environmental conditions with standard rat chow.

**Group I:** (Normal control): Received nothing.

**Group II:** (Dehydrated sham control): Dehydrated for 3 days.

**Group III:** (Dehydrated nebivolol administration): Dehydrated for 3 days and received nebivolol by oral rout for consecutive 5 days.

**Group IV:** (Dehydrated contrast medium administration): Dehydrated for 3 days and injected urografin intravenously into the tail vein at day 4.

**Group V:** (Dehydrated contrast medium and nebivolol administration): Dehydrated for 3 days and received nebivolol by oral rout for consecutive 5 days then injected urografin intravenously into the tail vein at day 4.

### Chemicals:

Urografin 76% (Ionic high- osmolar contrast medium meglumine/sodium diatrizoate) at a dose of 6 ml/kg body weight was administered intravenously into the tail vein at day 4 under ether anaesthesia.

Nebivolol tablets were given by oral gavage at a dose of 2 mg/kg body weight once daily for 5 days(days 1 to 5). Each tablet contains 5 mg nebivolol that was dissolved in 10 ml saline to obtain a final concentration of 0.5 mg/ml.

The experimental design and doses of chemicals were according to *Toprak et al. (2008)*

### Methods:

Twenty four hours after the last dose of nebivolol (day 6), the rats were sacrificed by cervical decapitation and dissected. The kidneys were excised and processed for either light microscopy (*Weiss et al., 2010*) or electron microscopy (*Woods and Stirling, 2008*).

## 3. Results:

### Histological and ultrastructural results:

#### Group I (normal control):

The renal cortex presented renal corpuscles, proximal convoluted tubules (PCT) and distal convoluted tubules (DCT) embedded in a scanty interstitial tissue. The renal corpuscle was formed of a spherical glomerulus invaginating into Bowman's capsule. The glomerulus was formed of a network of densely packed capillaries, surrounded by a clear

narrow urinary space limited by the flat squamous cells of the parietal layer of Bowman's capsule (Fig.1).

The renal medulla was formed of loops of Henle and collecting tubules embedded in abundant interstitial tissue. The loops of Henle were lined by simple cuboidal epithelial cells with scanty cytoplasm and apical nuclei bulging into the lumen, while the collecting tubules were lined by simple cuboidal to simple columnar epithelium (Fig.2).

Semithin sections of the renal cortex stained with toudine blue exhibited renal corpuscles, PCT and DCT. The cells of the PCT showed opposition of long apical brush borders of the surrounding cells with narrowing of the tubular lumen. The DCT featured shorter apical brush border and wider lumen (Fig.3). The renal medulla showed loops of Henle and collecting tubules (Fig.4).

Ultrastructural examination of the lining epithelium of PCT showed large rounded central nuclei with prominent nucleolus. There were abundant electron dense mitochondria with intact cristae in the basal parts of the cells between the nuclei and uniformly thick basal cell membranes with few electron- dense rounded lysosomes filled with dark homogenous matrix. Well developed long apical microvilli were also demonstrated and the cell exhibited basal processes surrounding the mitochondria in deep compartments; basal infoldings (Figs.5,6,7).

The lining epithelium of the medullary thick ascending limb of Henle (mTAL) showed large rounded central nuclei bulging into the lumen, abundant electron dense mitochondria with intact cristae distributed randomly in the cytoplasm and well developed long apical microvilli. A uniformly thin basal cell membrane and basal infolding were also demonstrated (Figs.8,9).

#### **Group II** (Dehydrated sham control):

Hematoxlin and eosin stained sections of the rat kidney of this group revealed glomerular capillary congestion. Some of the renal tubules were dilated and their lumen showed cast formation. Interstitial peritubular exudates in the medulla were visualized (Figs.10, 11).

Semithin sections stained with toudine blue exhibited shrunken glomeruli, widening of urinary space and capillary congestion. The renal tubules showed nuclear pyknosis, intraluminal exfoliation (detached epithelial lining cells), partial loss of the apical brush border and intraluminal casts formation. Interstitial tissue exudates could be demonstrated (Figs.12,13).

Electron microscopic examination of the epithelial lining cells of the PCT revealed nuclear changes in the form of margination of chromatin material. The mitochondria showed variability in size

and shape, enlargement (ballooning) with partial to complete loss of their cristae. There was partial loss of apical microvilli with vacuolations and rarefaction of the cytoplasm and loss of the basal infoldings (Figs.14,15).

The cells of the mTAL exhibited nuclear changes in the form of dissolution of chromatin material (kariolysis) and blebbing of nuclear membrane. The mitochondria were increased in number some were elongated and some were swollen with lost cristae. Areas of cytoplasmic rarefaction and partially damaged apical microvilli were visualized (Figs.16, 17).

#### **Group III** (Dehydrated nebivolol treated):

Light microscopic examination of rat kidney specimens of this group showed renal corpuscles formed of a glomerulus surrounded by a parietal layer of Bowman's capsule with a narrow urinary space in-between. Most of renal tubules appeared normal; few tubules were dilated (Figs.18, 19).

Semithin sections stained with tuloudine blue confirmed the previous findings. The glomeruli were either normal or mildly congested. Most of PCT and DCT featured an intact apical brush border. Few epithelial lining cells of renal tubules exhibited nuclear pyknosis (Figs.20,21).

Ultrastructural examination of the cells lining the PCT showed an intact apical microvilli, a uniformly thick basal cell membrane and intact basal infoldings. No evidence of mitochondrial affection was seen. Small areas of cytoplasmic rarefaction were demonstrated (Figs.22,23).

The cells of mTAL showed improvement of apoptotic changes, the nucleus appeared normal, intact apical microvilli and basal infoldings. Mitochondria appeared normal in size and shape (Fig.24).

#### **Group IV** (Dehydrated contrast medium treated):

Light microscopic examination of rat kidney specimens revealed shrinkage of glomeruli and widening of the urinary space. Most of renal tubules were abnormally dilated and showed casts in their lumina formed by detached cells and abnormal proteins. The cells lining these tubules were extensively vacuolated and their nuclei showed apoptotic like changes or pyknosis. Extravasated blood in-between renal tubules were observed (Figs.25, 26).

Semithin sections stained with toluidine blue revealed shrunken glomeruli with a widened urinary space. The renal tubules featured partial to complete loss of apical brush border, nuclear pyknosis, intraluminal casts formation and exfoliation. The cytoplasm showed extensive vacuolation. An interstitial tissue exudates were visualized (Figs.27,28).

Electron microscopic examination of the cells of the PCT revealed marked nuclear affection in the form of peripheral condensation of chromatin material with blebbing of nuclear envelope. The mitochondria showed marked increase in number, swelling with partial to complete loss of their cristae. Partial loss of apical microvilli and extensive cytoplasmic rarefaction were also encountered (Figs.29,30).

Ultrastructural examination of the cells of the mTAL illucidated lost tubular architecture, blebbing of nuclear envelope, lost basal infoldings, cytoplasmic rarefaction and increased number of mitochondria, most of them were swollen with partial or complete loss of their cristae (Figs. 31,32).

**Group V** (Dehydrated contrast medium and nebulol treated):

Light microscopic examination of rat kidney specimens of this group showed apparently normal renal corpuscles. Most of renal tubules appeared normal, few tubules were dilated (Figs.33,34).

Semithin sections stained with toluidine blue displayed either normal renal tubules or slightly damaged tubules with intraluminal exfoliation (Fig.35).

Ultrastructural examination of the lining epithelial cells of the PCT revealed abundant parallel electron dense mitochondria situated between the nucleus and a uniformly thick basal cell membrane. Intact apical microvilli were demonstrated (Fig.36).

The mTAL cells featured a normal nucleus, abundant electron dense mitochondria with intact cristae, intact basal infoldings and partially intact apical microvilli (Fig.37).

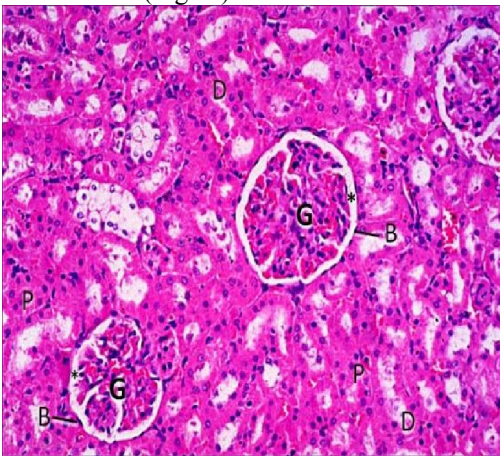


**Fig.1:** A photomicrograph of a cross section of the renal cortex of a rat of group I (Normal control) showing renal corpuscles, formed of a dense rounded glomerulus (G) surrounded by a parietal layer of Bowman's capsule (B) with the urinary space (\*) in-between. Proximal (P) and distal (D) convoluted tubules can be observed. Hx.&E.;X200

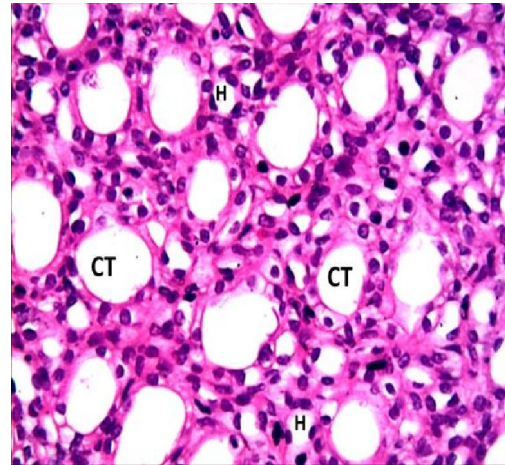


**Fig.2:** A photomicrograph of a cross section of the renal medulla of a rat of group I featuring collecting tubules (CT) lined with simple columnar epithelium and loops of Henle (H) lined with simple cuboidal epithelium with scanty cytoplasm and bulging nuclei into the lumen. Hx.&E.; X400

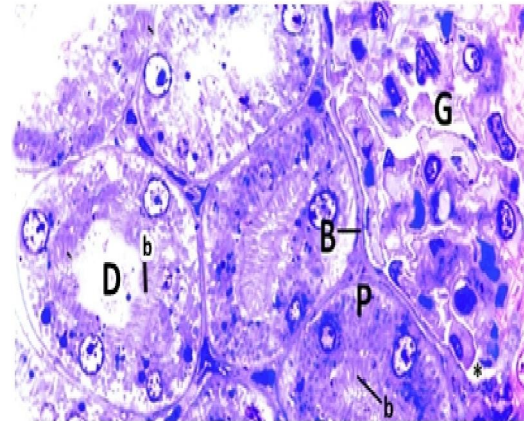


**Fig.3:** A photomicrograph of a semithin section of the renal cortex of a rat of group I demonstrating a renal corpuscle formed of a glomerulus (G) surrounded by a parietal layer of Bowman's capsule (B), with the urinary space (\*) in-between. A dense apical brush border (b) of both proximal (P) and distal (D) convoluted tubules can be seen. Toluidine blue; x 1000

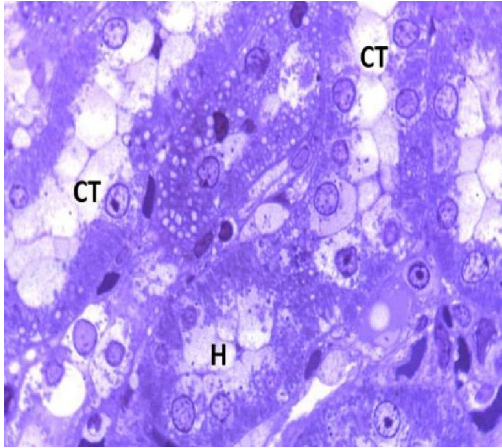


**Fig.4:** A photomicrograph of a semithin section of the renal medulla of a rat of group I showing collecting tubules (CT) lined with simple columnar epithelium and loops of Henle (H) lined with simple cuboidal epithelium with scanty cytoplasm and bulging nuclei into the lumen. Toluidine blue; x 1000

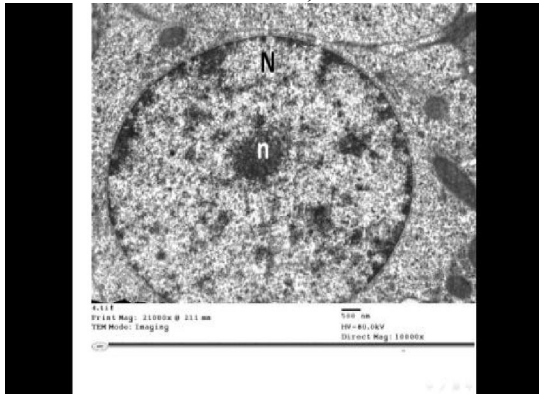


**Fig.5:** An electron micrograph of a rat kidney of group I displaying a proximal convoluted tubular cell with a rounded midpositioned nucleus (N) and a prominent nucleolus (n). x 10,000

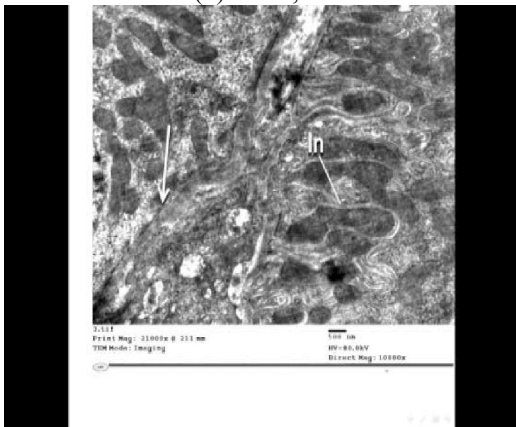


**Fig.6:** An electron micrograph of a rat kidney of group I displaying a proximal convoluted tubular cell with a uniformly thick basal cell membrane (white arrow) and intact basal infoldings (In). x 10,000

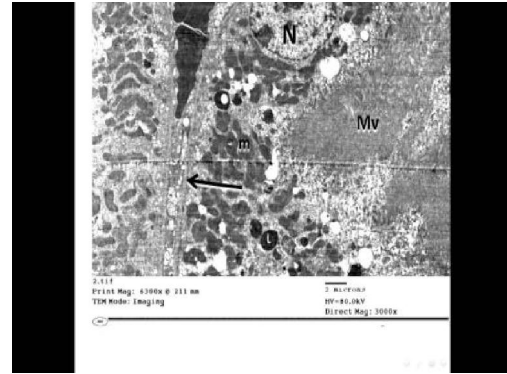


**Fig.7:** An electron micrograph of a rat kidney of group I displaying a proximal convoluted tubular cell with rounded mid positioned nucleus (N), few number of lysosomes (L), and abundant parallel electron dense mitochondria (m) are situated between the nucleus and a uniformly thick basal cell membrane (black arrow). Intact apical microvilli (Mv) can be observed. x 3,000

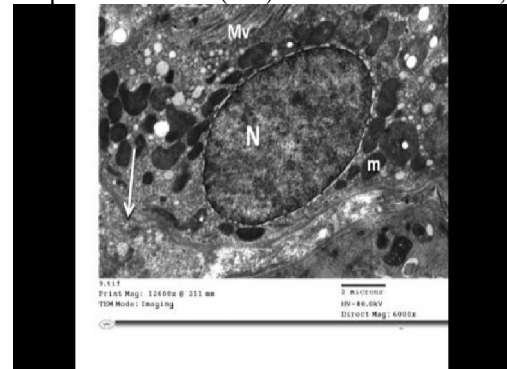


**Fig.8:** An electron micrograph of a rat kidney of group I displaying an epithelial lining cell of medullary thick ascending limb of Henle with bulging nucleus (N) into the lumen, intact apical microvilli (Mv), a uniformly thin basal cell membrane (white arrow) and abundant electron dense mitochondria (m) with intact cristae. x 6,000

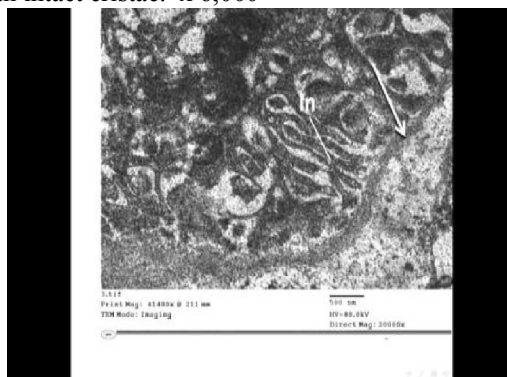


**Fig.9:** An electron micrograph of a rat kidney of group I displaying an epithelial lining cell of medullary thick ascending limb of Henle with a uniformly thin basal cell membrane (white arrow) and intact basal infoldings (In). x 20,000

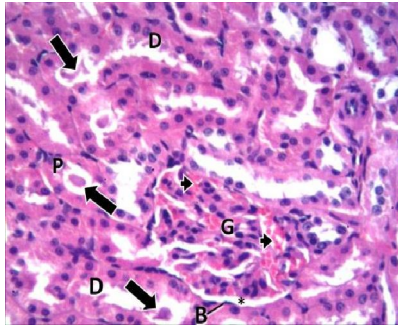


**Fig.10:** A photomicrograph of a cross section of the renal cortex of a rat of group II featuring proximal (P) and distal (D) convoluted tubules with intra-luminal casts (thick arrow). A glomerulus (G) exhibits capillary congestion (arrow head) surrounded by a parietal layer of Bowman's capsule (B) with the urinary space (\*) in-between. Hx.&E.; X 400

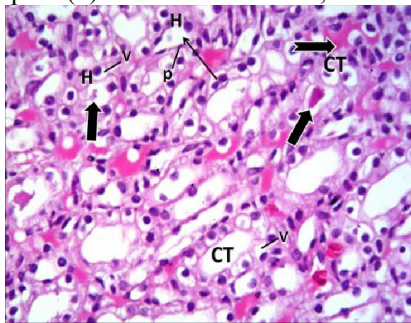


**Fig.11:** A photomicrograph of a cross section of the renal medulla of a rat of group II featuring vacuolations (v) and intra-luminal casts (thick arrow) of loop of Henle (H) and collecting tubules (CT). A loop of Henle exhibits dilated lumen (thin arrow) and nuclear pyknosis (p). Interstitial tissue exudates (notched arrow) can be observed. Hx.&E.;X 400

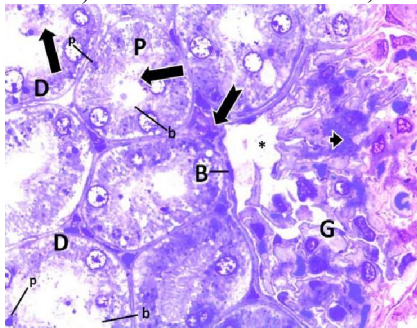


**Fig.12:** A photomicrograph of a semithin section of the renal cortex of a rat of group II demonstrating a shrunken glomerulus (G) with capillary congestion (arrow head) surrounded by a parietal layer of Bowman's capsule (B) with a widened urinary space (\*) in-between. The proximal (P) and distal (D) convoluted tubules feature a partially lost apical brush border (b), nuclear pyknosis (p) and intraluminal casts (thick arrow). An interstitial tissue exudates (notched arrow) can be seen. Toluidine blue;x 1000

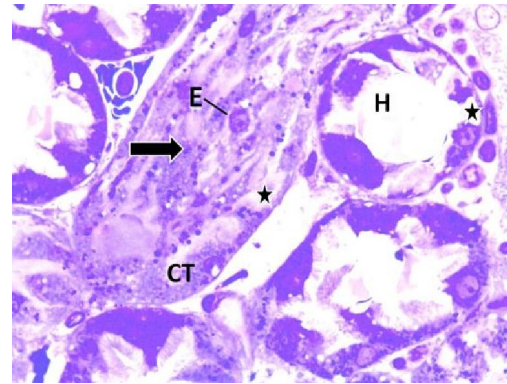


**Fig.13:** A photomicrograph of a semithin section of the renal medulla of a rat of group II demonstrating intraluminal casts (thick arrow) and exfoliation (E) of collecting tubule (CT). Detached cells (star) in the collecting tubules and loop of Henle (H) can be observed. Toluidine blue;x 1000

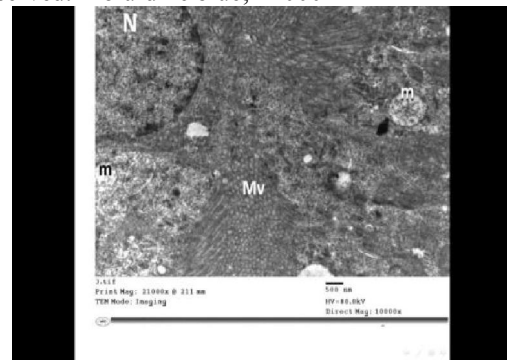


**Fig.14:** An electron micrograph of a rat kidney of group II showing a proximal convoluted tubular cell with margination of the chromatin material of nucleus (N), partially damaged apical microvilli (Mv) and swollen mitochondria (m) with partial or complete loss of cristae. x 10,000

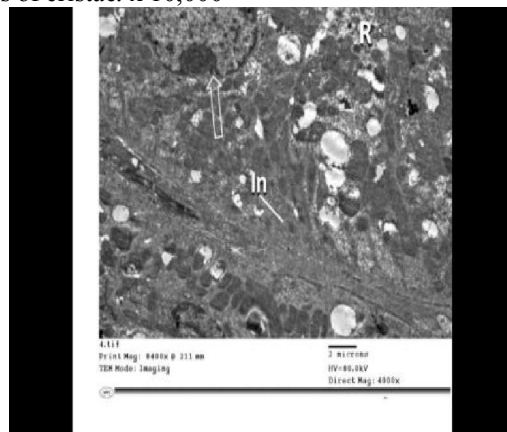


**Fig.15:** An electron micrograph of a rat kidney of group II displaying a proximal convoluted tubular cell with blebbing (transparent arrow) of nuclear envelope, lost basal infoldings (In) and rarefaction (R) of the cytoplasm. x 4,000

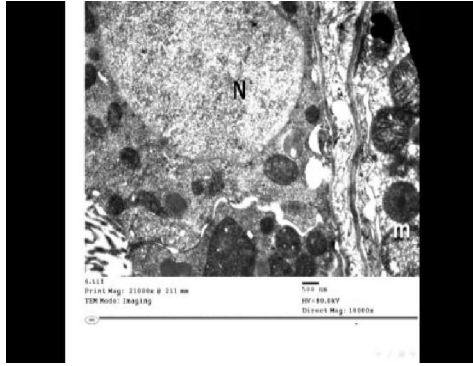


**Fig.16:** An electron micrograph of a rat kidney of group II featuring an epithelial lining cell of medullary thick ascending limb of Henle with complete dissolution of the chromatin material of the nucleus (N). Few swollen mitochondria (m) with lost cristae can be observed. x 10,000

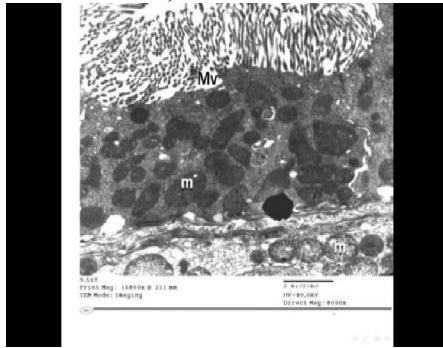


**Fig.17:** An electron micrograph of a rat kidney of group II displaying an epithelial lining cell of medullary thick ascending limb of Henle with partially damaged apical microvilli (Mv). Few mitochondria (m) are elongated and few are swollen with partial to complete loss of cristae. x 8,000

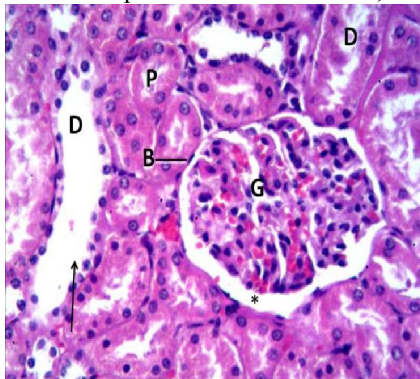


**Fig.18:** A photomicrograph of a cross section of the renal cortex of a rat of group III showing a renal corpuscle formed of a glomerulus (G) surrounded by a parietal layer of Bowman's capsule (B) with the urinary space (\*) in-between. Most of proximal (P) and distal (D) convoluted tubules are normal, a distal convoluted tubule is dilated (thin arrow). Hx.&E.; X 400

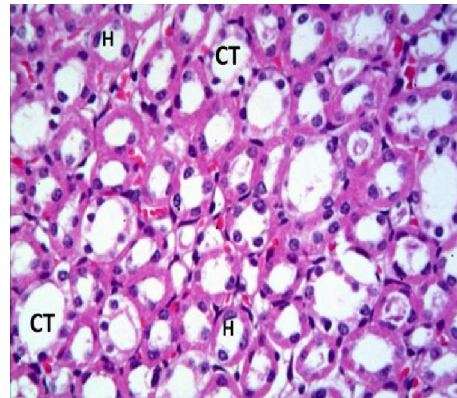


**Fig.19:** A photomicrograph of a cross section of the renal medulla of a rat of group III showing normal loops of Henle (H) and normal collecting tubules (CT). No vacuolations or interstitial tissue exudates can be seen. Hx.&E.;X 400

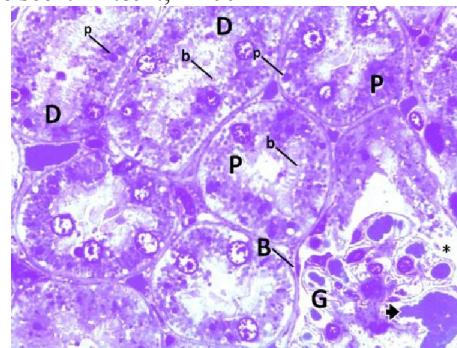


**Fig.20:** A photomicrograph of a semithin section of the renal cortex of a rat of group III demonstrating a glomerulus (G) with mild capillary congestion (arrow head) surrounded by a parietal layer of Bowman's capsule (B) with the urinary space (\*) in-between. Most of proximal (P) and distal (D) convoluted tubules feature an intact apical brush border (b). Few epithelial lining cells of renal tubules exhibit nuclear pyknosis (p). Toluidine blue;x 1000

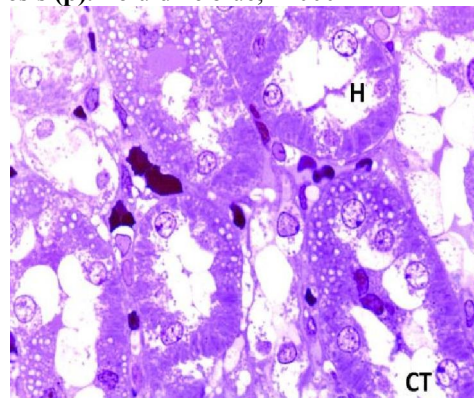


**Fig.21:** A photomicrograph of a semithin section of the renal medulla of a rat of group III demonstrating normal loops of Henle (H) and normal collecting tubules (CT). Toluidine blue;x 1000

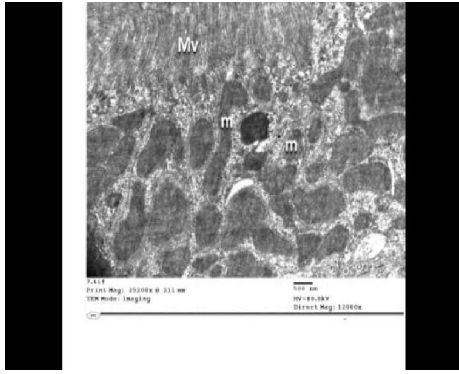


**Fig.22:** An electron micrograph of a rat kidney of group III displaying a proximal convoluted tubular cell with abundant parallel electron dense basal mitochondria (m), most of them are normal and few are elongated. Intact apical microvilli (Mv) can be observed. x 12,000

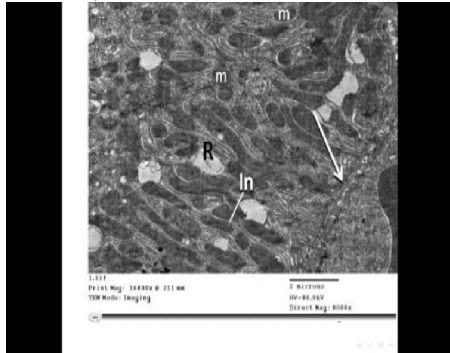


**Fig.23:** An electron micrograph of a rat kidney of group III displaying a proximal convoluted tubular cell with abundant parallel electron dense basal mitochondria (m), a uniformly thick basal cell membrane (white arrow) and intact basal infoldings (In). Small areas of rarefaction (R) can be demonstrated. x 8,000

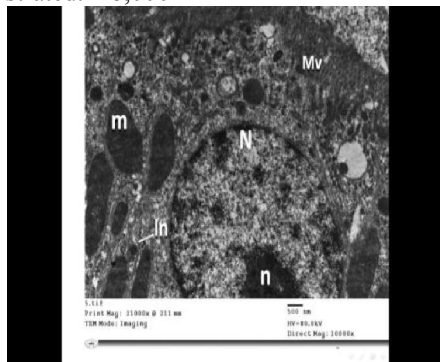


**Fig.24:** An electron micrograph of a rat kidney of group III showing an epithelial lining cell of medullary thick ascending limb of Henle with a normal nucleus (N) with a prominent nucleolus (n), intact basal infoldings (In) and electron dense mitochondria (m) with intact cristae. Intact apical microvilli (Mv) can be observed. x 10,000

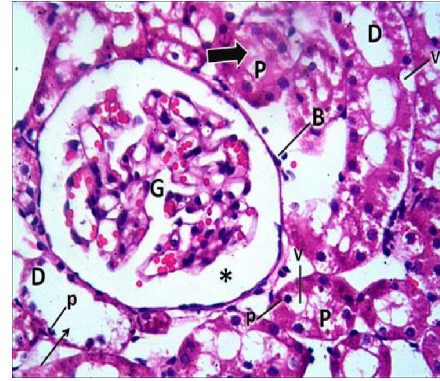


**Fig. 25:** A photomicrograph of a cross section of the renal cortex of a rat of group IV showing a shrunken glomerulus (G) surrounded by a parietal layer of Bowman's capsule (B) with widened urinary space (\*) in-between. Dilated (thin arrow) proximal (P) and distal (D) convoluted tubules that exhibit nuclear pyknosis (p) and vacuolations (v). Intraluminal casts (thick arrow) in the proximal convoluted tubules (P) can be observed. Hx.&E.; X 400

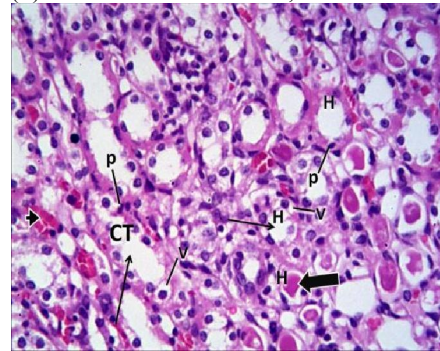


**Fig.26:** A photomicrograph of a cross section of the renal medulla of a rat of group IV showing dilated (thin arrow) loops of Henle (H) and collecting tubules (CT) with intraluminal casts (thick arrow), vacuolations (v) and nuclear pyknosis (p). Extravasated blood (arrow head) in-between renal tubules can be seen. Hx.&E.; X 400

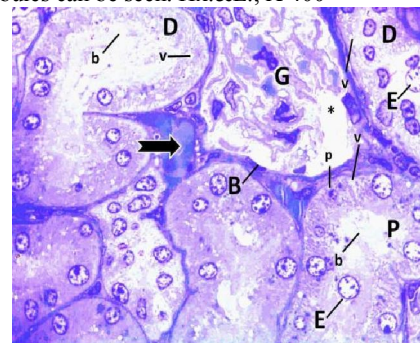


**Fig.27:** A photomicrograph of a semithin section of the renal cortex of a rat of group IV demonstrating a shrunken glomerulus (G) surrounded by a parietal layer of Bowman's capsule (B) with a widened urinary space (\*) in-between. The proximal (P) and distal (D) convoluted tubules feature a completely lost apical brush border (b), nuclear pyknosis (p), vacuolations (v) and intraluminal exfoliation (E). Interstitial tissue exudates (notched arrow) can be seen. Toluidine blue;x 1000



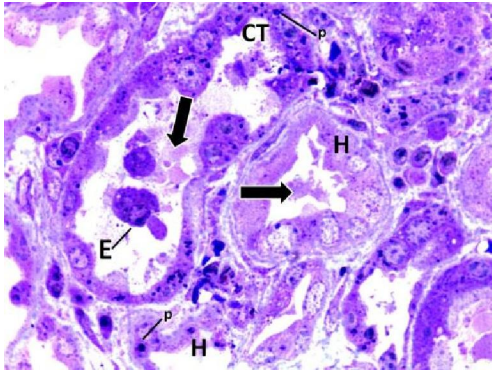


**Fig.28:** A photomicrograph of a semithin section of the renal medulla of a rat of group IV demonstrating collecting tubules (CT) and loops of Henle (H) with intraluminal casts (thick arrow), nuclear pyknosis (p) and intraluminal exfoliation (E). Toluidine blue;x 1000

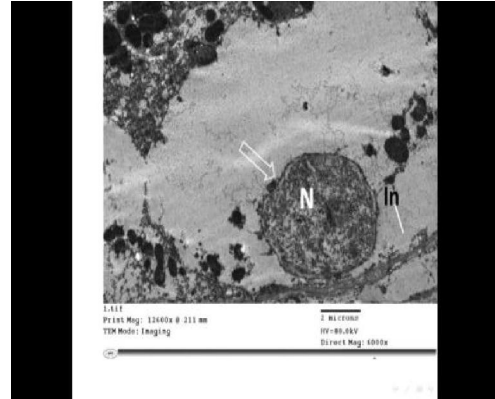


**Fig.31:** An electron micrograph of a rat kidney of group IV displaying an epithelial lining cell of medullary thick ascending limb of Henle with lost tubular architecture, blebbing (transparent arrow) of nuclear envelope and lost basal infoldings (In). x 6,000

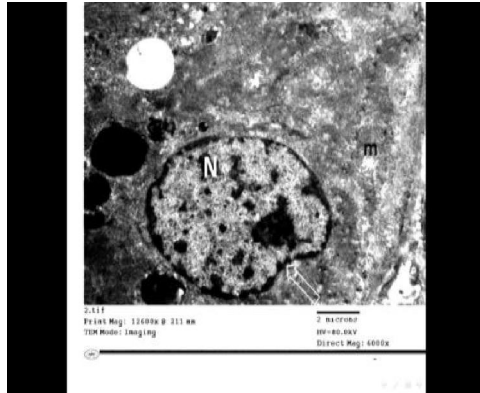


**Fig. 29:** An electron micrograph of a rat kidney of group IV displaying a proximal convoluted tubular cell with peripheral condensation of chromatin material of the nucleus (N), blebbing (transparent arrow) of nuclear envelope and swollen mitochondria (m) with lost cristae. x 6,000

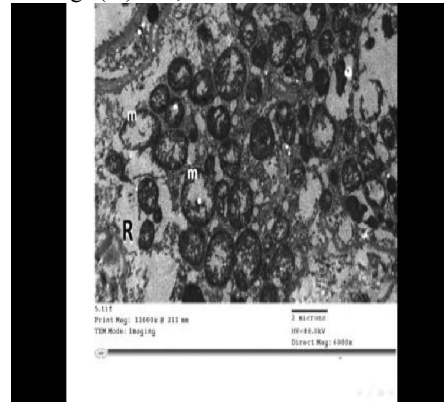


**Fig.32:** An electron micrograph of a rat kidney of group IV displaying an epithelial lining cell of medullary thick ascending limb of Henle with cytoplasmic rarefaction (R) and increased number of swollen mitochondria (m) with partial or complete loss of cristae. x 6,000

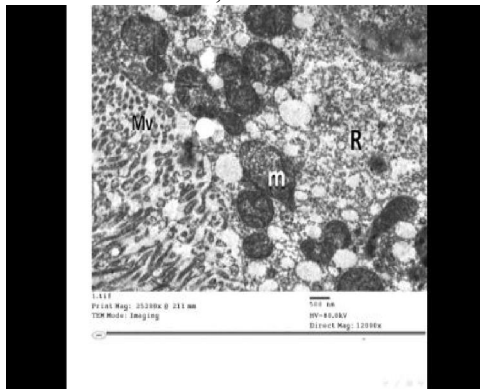


**Fig.30:** An electron micrograph of a rat kidney of group IV displaying a proximal convoluted tubular cell with swollen mitochondria (m) with lost cristae and extensive cytoplasmic rarefaction (R). Partially lost apical microvilli (Mv) can be demonstrated. x 12,000

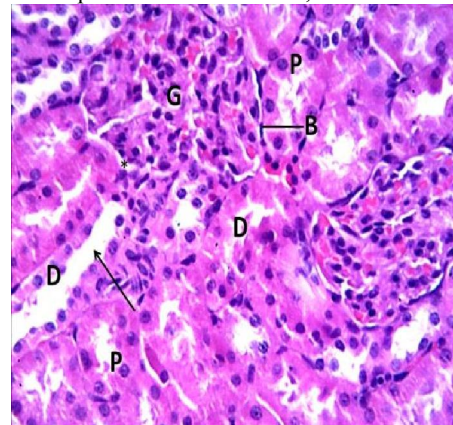


**Fig. 33:** A photomicrograph of a cross section of the renal cortex of a rat of group V showing a normal renal corpuscle, formed of dense rounded glomerulus (G) surrounded by a parietal layer of Bowman's capsule (B) with the urinary space (\*) in-between. Normal proximal (P) and distal (D) convoluted tubules can be observed and a distal convoluted tubule is dilated (thin arrow). Hx.&E.; X400

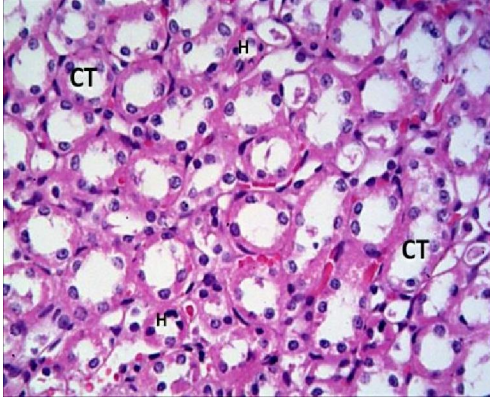


**Fig. 34:** A photomicrograph of a cross section of the renal medulla of a rat of group V showing normal collecting tubules (CT) and loops of Henle (H). Hx.&E.; X400

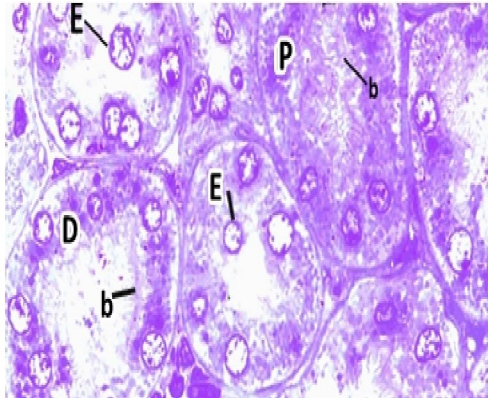


**Fig.35:** A photomicrograph of a semithin section of the renal cortex of a rat of group V demonstrating intact apical brush border (b) of the proximal (P) and distal (D) convoluted tubules. A proximal convoluted tubule exhibits intraluminal exfoliation (E) can be observed. Toluidine blue; x 1000

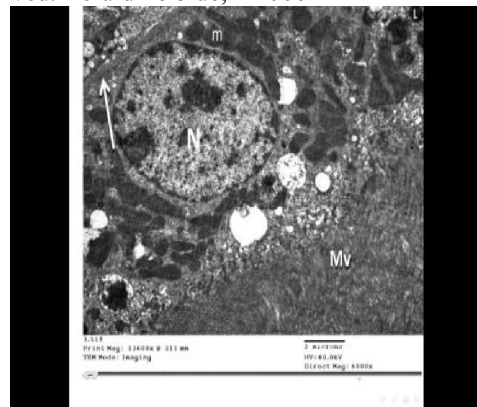


**Fig.36:** An electron micrograph of a rat kidney of group V displaying a proximal convoluted tubular cell with a uniformly thick basal cell membrane (white arrow), normal nucleus (N) and electron dense mitochondria (m). Intact apical microvilli (Mv) can be observed. x 6,000

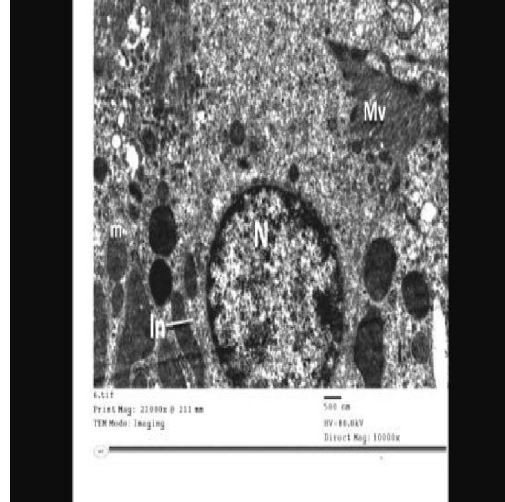


**Fig. 37:** An electron micrograph of a rat kidney of group V displaying an epithelial lining cell of medullary thick ascending limb of Henle with a normal nucleus (N), intact basal infoldings (In) and partially intact apical microvilli (Mv). Electron dense mitochondria (m) with intact cristae can be observed. x 10,000

#### 4. Discussion

In the current study, dehydration of rats was applied as a risk factor for induction of contrast-induced nephropathy (CIN); rats were deprived from water for 72 hours. *Fung et al. (2004)* suggested that under dehydrated conditions, the cells may lose up to 28% or more of their water volume. This undermines all cellular activities, including kidney cells. Consequently, the kidney retains metabolic waste products and cannot eliminate properly excessive drugs such as urografin augmenting its toxic effect. On the other hand, *Burchardt et al. (2013)* reported that impairment of renal functions 12–18 h after contrast agent administration was detected even when prophylactic hydration was used.

In the current work, dehydration in group II induced glomerular damage and cortical necrotic changes in the form of tubular atrophy. The medulla revealed similar findings in mTAL and the collecting tubules.

*Leh et al. (2011)* stated that tubular atrophy in the juxtamedullary cortex is closely associated with glomerular collapse and indicates glomerular hypoperfusion. The reduced flow through the proximal tubular system seemed to induce tubular atrophy.

*Legrand et al. (2008)* emphasized that the necrotic changes are attributed to acute ischaemia; microvascular dysfunction in acute ischaemia is related to an imbalance between vasoconstrictors, especially endothelin-1, and vasodilators especially nitric oxide (NO) leading to decreased renal oxygen

supply. These abnormalities in vascular reactivity have been associated with increases in intracellular  $\text{Ca}^{2+}$  that may also cause cell death by inducing the activation of proteases, phospholipases, and pro-apoptotic pathways. Similarly *Srichai et al. (2008)* suggested that ischemia or toxin-induced acute kidney injury is generally thought to affect the cells of the proximal tubule.

In the present work, intraluminal epithelial casts were observed in rats of group II. *Miner et al. (2004)* reported that formation of tubular epithelial casts in dehydration is due to ischemic effect of vasopressin hormone released with consequent sloughing and detachment of renal tubular epithelial cells.

Partial loss of apical brush border was evident in this study. This was in agreement with *Bonventre and Weinberg (2003)* who suggested that ischemia results in rapid loss of cytoskeletal integrity and cell polarity; the microvilli disappear with shedding and internalization of apical membrane proteins. This was attributed to actin depolymerizing factor which is activated by dephosphorylation and redistributes from the cytosol to damaged microvilli, where it can promote depolymerization of actin.

In the current study, interstitial tissue exudates were found both in the cortex and the medulla. This was in accordance with *Vakkila and Lotze (2004)* who stated that necrosis is associated with pathological cell loss and the ability of necrotic cells to promote local inflammation.

Ultrastructural examination of the PCT and the mTAL revealed various degrees of nuclear affection, cellular apoptosis, partial damage of apical microvilli and loss of basal infoldings of the tubular basement membrane. Similar findings were reported by *Olsen et al. (1989)* and *Srichai et al. (2008)*.

In the present work, mitochondrial swelling with partial to complete loss of cristae were found. *Whiteman et al. (2008)* and *Szeto et al. (2011)* stated that altered mitochondrial membrane permeability leads to an osmotic imbalance that induces the swelling and lost cristae of the mitochondria. Furthermore, activated neutrophils release hydrogen peroxide and produce hypochlorous acid, which has been shown to cause mitochondrial dysfunction and cell death.

Cytoplasmic vacuolations were observed in group II of the present study. This was in accordance with *Baehrecke (2005)* who described that apoptosis involves activation of catabolic enzymes in which parts of the cytoplasm are sequestered within double-membraned vacuoles and finally digested by lysosomal hydrolases, cells deprived from exogenous energy sources catabolize part of their cytoplasm to

generate ATP and other intermediate metabolites that allow them to meet their essential energetic demand.

In the current study, administration of nebivolol to rats of group III revealed partial improvement of the previous findings as demonstrated by normal renal corpuscles and slight tubular degenerative changes. These findings were supported by ultrastructural examination of the PCT and mTAL. Similar findings have been recorded by *Toprak et al. (2008)* who reported that five days treatment with nebivolol attenuated the development of proteinaceous casts which developed secondary to dehydration.

In the present work, light microscopic examination of rat kidney specimens of dehydrated contrast medium administration group (Group IV) revealed ischemic collapse of most of glomeruli with secondary widening of urinary space and severely affected renal tubules. Similar pathological changes were observed in the renal medullary tubules especially the mTAL. Interstitial tissue exudates in the renal medulla were also found. These findings were confirmed by ultrastructural examination of the PCT and the mTAL. Similar findings in renal tubules were observed by *Toprak et al. (2008)* in their study in which the same dose of urografin was injected in rats and revealed tubular necrosis, especially in the outer zone of the medulla, proteinaceous casts and medullary congestion. *Caglar et al. (2001)* demonstrated that *in vivo* administration of radiocontrast agents resulted in proximal tubular vacuolar changes and brush border simplification (loss of microvilli). On the other hand, electron microscopical pictures in animal models of CIN revealed that the vacuolar changes were in fact basolateral membrane outpouchings with otherwise intact cellular structures (*Heyman et al., 1988*).

In the present work, most of the renal tubules in group IV were severely affected, especially the PCT and mTAL. *Sarafidis et al. (2006)* suggested that PCT cells are especially affected by urografin owing to their high oxygen consumption; they are the most metabolically active renal cells, so they are commonly affected by toxins and ischemia.

*Detrenis et al. (2005)* reported that reduction in renal plasma flow is not uniform and occurs especially in the medulla, since medullary perfusion and partial  $\text{O}_2$  pressure ( $\text{PO}_2$ ) are much lower than in the cortex. The mTAL is characterized by high metabolic activity and increased  $\text{O}_2$  demand due to active ion transport through the membrane. Therefore, renal hypoxia may be a critical factor in the pathogenesis of CIN. Contrast media induce potential osmotic diuresis and can cause an increased energy need in the mTAL.

*O'Donnell et al. (2010)* stated that increased osmolarity of contrast media has been found to directly induce DNA fragmentation of renal epithelial

cells. *Itoh et al. (2006)* reported that the toxic effects of contrast media may include cellular energy failure, a disruption of calcium homeostasis, a disturbance of tubular cell polarity and cell apoptosis. *Romano et al. (2008)* suggested that contrast media cause a marked increase in caspase-3 and -9 activities and poly(ADP-ribose) fragmentation in renal tubular cells, indicating that the contrast media activate apoptosis mainly through an intrinsic or mitochondrial pathway.

Tubular dilatation and acute obstructive nephropathy due to precipitation of urinary glycoprotein-contrast complexes in the renal tubules have been postulated by *Dawson et al. (1984)* to explain the episodes of renal failure occasionally seen following intravascular contrast medium administration.

In the present work, intraluminal casts were found in cortical and medullary tubules of group IV rats' kidney. *Hosojima et al. (2009)* reported that albuminuria and intraluminal cast formation are common after injection of urografin due to decreased expression of a protein receptor, megalin, via release of angiotensin- II. Megalin is a protein responsible for albumin uptake present in apical brush border of the PCT. Extravasation of blood was observed in-between renal tubules in this group. This was attributed by *Miner et al. (2004)* to accumulation of toxins secondary to the dehydration of rats; these toxins cause damage of blood vessels with subsequent erosion and haemorrhage.

Extensive cytoplasmic vacuolation was evident in rats of group IV probably due to disturbance of sodium pump impaired by oxidative phosphorylation that results in hydropic degeneration as justified by *Morcos et al. (1996)* who reported that cytoplasmic vacuolations may be due to active internalization of urografin in the cells of renal tubules leading to lysosomal changes. Extravasated blood in-between renal tubules in the medulla was found in group IV supposedly due to reperfusion injury. This is confirmed by *Sutton (2009)* who reported that reperfusion is associated with microvascular congestion and trapping of erythrocytes in the inner medullary region. The trapping of blood cells is thought to be due to loss of endothelial cell-to-cell contact, increased microvascular permeability, breakdown of the perivascular matrix and increased vascular reactivity.

Treatment with nebivolol for 5 days improved these severe degenerative changes. The rats of group V showed a partially intact apical brush border, the cytoplasm became densely acidophilic, tubular casts markedly decreased and mitochondrial affection was mild. These findings were in accordance with the work performed by *Hayden et al. (2010)* who stated that nebivolol has a renoprotective effect in a

transgenic rat model with hypertension and increased angiotensin II level due to its vasodilator properties and antioxidant effect.

In nebivolol treated group, nuclear affection and cell apoptosis were markedly improved probably due to its vasodilator effect of nebivolol with subsequent increase in renal blood flow and regeneration of renal tubules. This is confirmed by *Gori and Parker (2008)* who stated that compound mechanisms, including NO, prostaglandins and adenosine, continuously adjust medullary tubular transport activity to the limited available oxygen supply. Furthermore, *Whaley-Connell et al. (2009)* reported that treatment with nebivolol for 3 weeks reduced tubulointerstitial oxidative stress and fibrosis as well as PCT structural abnormalities in addition to reduced urinary albumin.

In the present work nebivolol administration markedly improved mitochondrial structure. This was in accordance with *Hayden et al. (2010)* who stated that nebivolol treatment improved mitochondrial structure and reduced NADPH oxidase activity. The rapid recovery of ATP appears to protect the microvascular endothelial cell and dramatically reduces microvascular congestion, providing better reflow to the medulla and improved creatinine clearance.

In the current study, dehydration was a precipitating factor for development of CIN. So, it is mandatory to perform a periprocedural hydration of the patient by intravenous saline administration. Concomitant administration of nebivolol afford a partial protection against urografin-induced nephrotoxicity due to its vasodilator and antioxidant effects.

## References

1. *Avcı, E., Yeşil, M., Bayata, S., Postacı, N.; Arıkan, E. and Cirit, M. 2011.* The role of nebivolol in the prevention of contrast-induced nephropathy in patients with renal dysfunction. The Anatolian Journal of Cardiology 11(7):613-617.
2. *Baehrecke, E.H. 2005:* Autophagy: dual roles in life and death? Nature Reviews Molecular Cell Biology 6: 505-510.
3. *Bonventre, J.V. and Weinberg, J.M. 2003.* Recent Advances in the Pathophysiology of Ischemic Acute Renal Failure. Journal of The American Society of Nephrology 14 (8): 2199-2210.
4. *Brendan, J., Barrett, M.B., Patrick, S. and Parfrey, M.D. 2006.* Preventing nephropathy induced by contrast media. New England. Journal of Medicine 354:379-386.
5. *Burchardt, P., Guzik, P., Tabaczewski, P., Synowiec, T., Bogdan, M., Faner, P., Chmielarczyk-Sobocińska, A., Palasz, A. 2013.* Early renal dysfunction after contrast media administration

- despite prophylactic hydration. The International Journal of Cardiovascular Imaging 29(5): 959–966.
6. **Caglar, Y., Mete, U.O. and Kaya, M. 2001.** Ultrastructural evaluation of the effects of the contrast media on the rat kidney. Journal of Submicroscopic Cytology and Pathology 33:443-451.
  7. **Dawson, P., Freedman, D., Howell, M. and Hine, A.L. 1984.** Contrast-medium-induced acute renal failure and Tamm-Horsfall proteinuria. British Journal of Radiology 57:577-579.
  8. **Detrenis, S., Meschi, M. and Musini, S. 2005.** Lights and shadows on the pathogenesis of contrast-induced nephropathy: state of the art. Nephrology Dialysis Transplantation 20:1542-1550.
  9. **Fishbane, S., Durham, J., Marzo, K. and Rundick, M. 2004.** N-Acetylcysteine in the prevention of radiocontrast-induced nephropathy. Journal of the American Society of Nephrology 15:251-261.
  10. **Fung, J., Szeto, C., Chan, W., Kum, L., Chan, A., Wong, J., Yip, G., Chan, J., Yu, C., Woo, K. and Sanderson, J. 2004.** Effect of N-acetylcysteine for prevention of contrast nephropathy in patients with moderate to severe renal insufficiency: a randomized trial. American Journal of Kidney Diseases 43: 801–808.
  11. **Gori, T. and Parker, J.D. 2008.** Nitrate-induced toxicity and preconditioning: a rationale for reconsidering the use of these drugs. Journal of American College of Cardiology 52: 251-254.
  12. **Gupta, S. and Wright, H.M. 2008.** Nebivolol: a highly selective beta1-adrenergic receptor blocker that causes vasodilation by increasing nitric oxide. Cardiovascular Therapeutics 26(3):189-202.
  13. **Hayden, M. R., Habibi, J., Whaley-Connell, A., Johnson, M., Tilmon, R., Jain, D., Ferrario, C. and Sowers, J.R. 2010.** Nebivolol Attenuates Maladaptive Proximal Tubule Remodeling in Transgenic Rats. American Journal of Nephrology 31(3): 262–272.
  14. **Heyman, S.N., Brezis, M., Reubinoff, C.A., Greenfeld, Z., Lechene, C., Epstein, F. and Rosen, S. 1988.** Acute renal failure with selective medullary injury in the rat. Journal of Clinical Investigation 82:401–412.
  15. **Hosojima, M., Sato, H., Yamamoto, K., Kaseda, R., Soma, T., Kobayashi, A., Suzuki, A., Kabasawa, H., Takeyama, A., Ikuyama, K., Iino, N., Nishiyama, A., Thekkumkara, T.J., Takeda, T., Suzuki, Y., Gejyo, F. and Saito, A. 2009.** Regulation of megalin expression in cultured proximal tubule cells by angiotensin II type 1A receptor- and insulin-mediated signaling cross talk. Endocrinology 150:871–878.
  16. **Huang, X., Yoshikoshi, A., Hirano, K. and Sakanishi, A. 2003.** Effects of contrast media on erythrocyte aggregation during sedimentation. Canadian Journal of Physiology and Pharmacology 81(4):397-404.
  17. **Itoh, Y., Yano, T., Sendo, T., Sueyasu, M., Hirano, K., Kanaide, H. and Oishi, R. 2006.** Involvement of de novo ceramide synthesis in radiocontrast-induced renal tubular cell injury. Kidney International 69:288-297.
  18. **Jo, S.H., Koo, B.K., Park, J.S., Kang, H.J., Kim, Y.J., Kim, H.L., Chae, I.H., Choi, D.J., Sohn, D.W., Oh, B.H., Park, Y.B., Choi, Y.S. and Kim, H.S. 2009.** N-acetylcysteine versus Ascorbic acid for preventing contrast-Induced nephropathy in patients with renal insufficiency undergoing coronary angiography NASPI study-a prospective randomized controlled trial. American Heart Journal 157(3):576-583.
  19. **Larner, S.F., Hayes, R.L. and Wang, K.K. 2006.** Unfolded protein response after neurotrauma. Journal of Neurotrauma 23:807-829.
  20. **Legrand, M., Mik, E.G., Johannes, T., Payen, D. and Ince, C. 2008.** Renal Hypoxia and Dysoxia After Reperfusion of the Ischemic Kidney. Molecular Medicine 14: 502–516.
  21. **Leh, S., Hultström, M., Rosenberger, C. and Iversen, B. 2011.** Afferent arteriopathy and glomerular collapse but not segmental sclerosis induce tubular atrophy in old spontaneously hypertensive rats. Virchows Archiv 459(1): 99–108.
  22. **Mason, R.P., Kubant, R. and Jacob, R.F. 2006.** Effect of nebivolol on endothelial NO and peroxynitrite release in hypertensive animals: Role of antioxidant activity. Journal of Cardiovascular Pharmacology 48:862-869.
  23. **Merten, G.J., Burgess, W.P., Gray, L.V., Holleman, J.H., Roush, T.S., Kowalchuk, G.J., Bersin, R.M., Van Moore, A., Simonton, C.A., Rittase, R.A., Norton, H.J. and Kennedy, T.P. 2004.** Prevention of contrast-induced nephropathy with sodium bicarbonate: a randomized controlled trial. The Journal of the American Medical Association 291: 2328–2334
  24. **Miner, S., Dzavik, V., Nguyen, P., Richardson, R., Mitchell, J., Atchison, D., Seidelin, P., Daly, P., Ross, J., McLaughlin, P., Ing, D., Lewycky, P., Barolet, A. and Schwartz, L. 2004.** N-Acetylcysteine reduces contrast-associated nephropathy but not clinical events during long-term follow-up. American Heart Journal 148: 690–695.
  25. **Morcos, S., Epstein, F., Haylor, J. and Dabrota, M. 1996.** Aspects of contrast media nephrotoxicity. European Journal of Radiology 23: 178 184.
  26. **Mueller, C., Buerkle, G., Perruchoud, A.P. and Buettner, H.J. 2004.** Female sex and risk of contrast nephropathy after percutaneous coronary intervention. The Canadian Journal of Cardiology 20(5):505-509.

27. **O'Donnell, D.H., Moloney, M.A., Bouchier-Hayes, D.J. and Lee, M.J. 2010.** Contrast-Induced Nephrotoxicity, Possible Synergistic Effect of Stress Hyperglycemia. *American Journal of Roentgenology* 195:45-49.
28. **Olsen, S., Burdick, J.F., Keown, P.A., Wallace, A.C., Racusen, L.C. and Solez, K. 1989.** Primary acute renal failure (acute tubular necrosis) in the transplanted kidney: morphology and pathogenesis. *Medicine (Baltimore)* 68(3):173-187.
29. **Persson, P.B., Hansell, P. and Liss, P. 2005.** Pathophysiology of contrast medium-induced nephropathy. *Kidney International* 68: 14-22.
30. **Romano, G., Briguori, C., Quintavalle, C., Zanca, C., Rivera, N.V., Colombo, A. and Condorelli, G. 2008.** Contrast agents and renal cell apoptosis. *European Heart Journal* 29:2569-2576.
31. **Santos, R.O., Malvar, B., Silva, R., Ramalho, V., Pessegueiro, P., Amoedo, M., Aniceto, J., Pires, C. 2011.** Contrast-induced nephropathy. *Acta Medica Portuguesa* 24(5):809-820.
32. **Sarafidis, P., Whaley-Connell, A., Sowers, J. and Bakris, G. 2006.** Cardiometabolic syndrome and chronic kidney disease: what is the link? *Journal of The Cardiometabolic Syndrome* 1(1): 58-65.
33. **Schweiger, M., Chambers, C., Davidson, C., Blankenship, J., Bhalla, N.P., Block, P.C., Dervan, J.P., Gasperetti, C., Gerber, L., Kleiman, N.S., Krone, R.J., Phillips, W.J., Siegel, R.M., Uretsky, B.F., Laskey, W.K. 2007.** Prevention of contrast induced nephropathy: Recommendations for the high risk patient undergoing cardiovascular procedures. *Catheterization and Cardiovascular Interventions* 69: 135-140.
34. **Srichai, M.B., Hao, C., Davis, L., Golovin, A.; Zhao, M.; Moeckel, G., Dunn, S., Bulus, N., Harris, R.C., Zent, R. and Breyer, M.D. 2008.** Apoptosis of the thick ascending limb results in acute kidney injury. *Journal of the American Society of Nephrology* 19(8):1538-46.
35. **Sutton, T.A. 2009.** Alteration of microvascular permeability in acute kidney injury. *Microvascular Research* 77: 4-7.
36. **Szeto, H.H., Liu, S., Soong, Y., Wu, D., Darrah, S., Cheng, F., Zhao, Z., Ganger, M., Tow, C. and Seshan, S. 2011.** Mitochondria-Targeted Peptide Accelerates ATP Recovery and Reduces Ischemic Kidney Injury. *Journal of The American Society of Nephrology* 22(6): 1041-1052.
37. **Teplan, V. 2012.** Contrast nephropathy and prevention. *Vnitřní Lekarství* 58(7-8): 553-556.
38. **Toblli, E., Cao, G., Giani, J.F., Muñoz, M. C., Angerosa, M. and Dominici, F. P. 2011.** Long-term treatment with nebivolol attenuates renal damage in Zucker diabetic fatty rats. *Journal of Hypertension*. 29:1613-1623.
39. **Toprak, O., Cirit, M., Tanrısev, M., Yazıcı, C., Canoz, O., Sipahioglu, M., Uzum, A., Ersoy, R. and Sozmen, E.Y. 2008.** Preventive effect of nebivolol on contrast-induced nephropathy in rats. *Nephrology Dialysis Transplantation* 23 (3): 853-859.
40. **Vakkila, J. and Lotze, M. 2004.** Inflammation and necrosis promote tumor growth. *Nature Reviews Immunology* 4: 641-648.
41. *Vnitřní Lekarství* 58(7-8):553-6.
42. **Weiss, A., Delcour, N., Meyer, A. and Klopffleisch, R. 2010.** Efficient and Cost-Effective Extraction of Genomic DNA From Formalin-Fixed and Paraffin-Embedded Tissues. *Veterinary Pathology* 227 (4): 834-838.
43. **Whaley-Connell, A., Habibi, J., Johnson, M., Timon, R., Rehmer, N., Rehmer, J., Wiedmeyer, C., Ferrario, C.M. and Sowers, J.R. 2009.** Nebivolol reduces proteinuria and renal NADPH oxidase-generated reactive oxygen species in the transgenic Ren2 rat. *American Journal of Nephrology* 30:354-360.
44. **Whiteman, M., Spencer, J.P., Szeto, H.H. and Armstrong, J.S. 2008.** Do mitochondriotropic antioxidants prevent chlorinative stress-induced mitochondrial and cellular injury? *Antioxidants & Redox. Signaling* 10: 641-650.
45. **Wong, P.C., Li, Z., Guo, J. and Zhang, A. 2012.** Pathophysiology of contrast-induced nephropathy. *International Journal of Cardiology* 158(2):186-192.
46. **Woods, A. and Stirling, J. 2008.** Electron microscopy. *Theory and Practice of Histological Techniques*. 6<sup>th</sup> edition, Churchill Livingstone, London, 601-640.